ELSEVIER

Journal of Fluids and Structures 19 (2004) 221–237

JOURNAL OF FLUIDS AND STRUCTURES

www.elsevier.nl/locate/jnlabr/yjfls

On the parametric excitation of some nonlinear aeroelastic oscillators

H. Lumbantobing[a], T.I. Haaker[b,*]

[a] *Department of Applied Mathematical Analysis, Faculty of Electrical Engineering, Mathematics and Computer Science Delft University of Technology, Mekelweg 4, 2628 CD Delft, The Netherlands*

[b] *Telematica Instituut, P.O. Box 589, 7500 AN Enschede, The Netherlands*

Received 4 March 2003; accepted 11 December 2003

Abstract

In this paper the parametric excitation of two one-degree-of-freedom nonlinear aeroelastic oscillators in cross-flow is considered. This is for example relevant for the understanding of aeroelastic oscillations of bridge stay cables induced by bridge deck motion. In particular the parametric excitation for a plunge oscillator and a seesaw oscillator are discussed. The following model equation for the parametric excitation of the aeroelastic oscillators is considered: $\ddot{z} + 2\beta\dot{z} + [1 - \kappa\cos(\omega t)]z = F(z, \dot{z}, U)$. Here, for the plunge oscillator, z denotes the vertical displacement of a mass-spring-damper system, and for the seesaw oscillator, z denotes the rotation of a seesaw structure around the hinge axis. F represents the nonlinear aeroelastic force which depends on z, $\dot{z}$ and wind velocity U. Assuming F, the coefficients of parametric excitation κ and structural damping β to be small, the averaging method can be applied to study the equation that equation. Note that it is a nonlinear Mathieu equation. Without the parametric excitation one typically finds an aerodynamic instability for a critical wind velocity above which finite amplitude, periodic oscillations result. The parametric excitation complicates this simple picture, especially for the seesaw oscillator. Depending on the ratio of κ and β a critical wind velocity may still exist. For some cases though, increasing the wind velocity above the critical velocity re-stabilizes the trivial solution. Next to the familiar periodic constant amplitude solutions also solutions with periodically modulated amplitudes and phases are obtained. Criteria for the stability of the trivial solution, the existence and the stability of various nontrivial (periodic) solutions and their bifurcations are given.

Keywords: Aeroelasticity; Nonlinear oscillation; Parametric excitation, Averaging; Bifurcation analysis

1. Introduction

This paper is concerned with the parametric excitation of two aeroelastic oscillators, plunge and seesaw oscillators, placed in a homogeneous and uniform wind flow. A schematic sketch of the plunge oscillator and the seesaw oscillator is given in Figs. 1 and 2, respectively.

The first oscillator is a spring supported cylinder with linear damping. It is restricted to oscillate perpendicular to the flow direction. If the cylinder has a non-circular cross section and is exposed to a homogeneous and uniform wind flow, self-excited so called galloping oscillations may arise, see Blevins (1990). Here we assume that the spring supporting the cylinder has a periodically varying stiffness, causing a parametric excitation, see Fig. 1.

*Corresponding author.
E-mail address: timber.haaker@telin.nl (T.I. Haaker).

0889-9746/$ - see front matter © 2003 Elsevier Ltd. All rights reserved.
doi:10.1016/j.jfluidstructs.2003.12.006

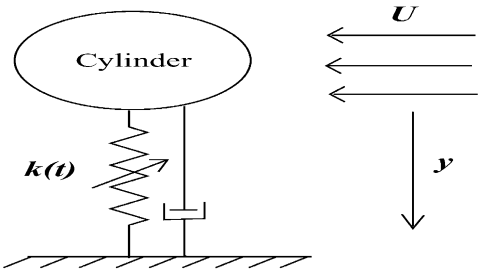

Fig. 1. Schematic sketch of the structure of the plunge oscillator.

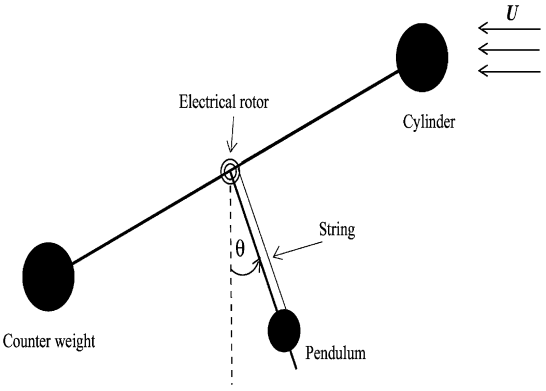

Fig. 2. Schematic sketch of the structure of the seesaw oscillator with an electrical rotor.

The second oscillator is a seesaw like structure consisting of a rigid bar hinged around an axis. The bar holds at its right end a cylinder. On the other end a counter weight is fixed balancing the cylinder with respect to the hinge axis. A pendulum weight fixed to the bar provides for a restoring moment. Again self-excited galloping oscillations may arise. In addition an electrical rotor is mounted on the hinge axis and connected to the pendulum weight via a string. The rotor causes the pendulum weight to slide periodically up and down the arm holding the pendulum, see Fig. 2. In the model equation this sliding pendulum weight causes a parametric excitation, see for example Van der Burgh (1996).

The main purpose of this paper is to study the influence of a parametric excitation on the well-known aeroelastic behaviour of the plunge and the seesaw oscillators. Such a study is relevant for the understanding of the aeroelastic behaviour of coupled structural elements exposed to wind flow. For example, Da Costa et al. (1996) studied the oscillations of bridge deck or bridge towers. They suggested parametric excitation as the driving mechanism. As a model equation they found a nonlinear Mathieu equation. They found that the most dangerous situations arise when the frequency of the parametric excitation is close to one or two times the natural frequency. Haaker and Van der Burgh (1994) modelled and analyzed the equation of motion of the seesaw oscillator for low flow velocities. The wind forces then act as a perturbation on the linear Hamiltonian system modelling the unforced oscillations of the seesaw structure for small amplitudes. Van Oudheusden (1996) investigated the galloping oscillations with a single rotational degree of freedom under the combined effect of both viscous and frictional damping. He studied how the additional effect of even slight amounts of frictional damping affects the galloping curve. He provided results from wind tunnel experiments that confirm the major findings of analysis. Lumbantobing and Haaker (2000, 2002a) considered the aeroelastic oscillations of a single seesaw and seesaw type oscillators under strong wind conditions. Tondl et al. (2000) considered parametric excitations for general oscillators with special nonlinear damping. They applied the averaging method to study the stability of the trivial solution. Lumbantobing and Haaker (2002b) considered the parametric excitation of a nonlinear aeroelastic seesaw oscillator. They applied the averaging method to study the behaviour of the trivial and the nontrivial solutions. Here we consider parametric excitation for a plunge oscillator and a seesaw oscillator, respectively. The model equation we obtain is a nonlinear Mathieu equation. To study the behaviour of the solutions of this equation we apply the averaging method.

This paper is organized as follows. In Section 2 the parametric excitation of the nonlinear aeroelastic plunge oscillator is considered. The analysis is started with the derivation of the model equation in Section 2.1 and then followed by the

analysis of the model equation in Section 2.2. The analysis of the model equation for the linear case is presented in section 2.2.1 and for the nonlinear case is presented in Section 2.2.2. In Section 2.2.3, some phase portraits for the averaged equations are presented. In Section 3 the parametric excitation of the nonlinear aeroelastic seesaw oscillator is considered. The derivation of the model equation for the aeroelastic response of the seesaw oscillator with parametric excitation is given in Section 3.1. The analysis of this equation is presented in Section 3.2, first the linear analysis in Section 3.2.1 and then the nonlinear analysis in Section 3.2.2. In Section 3.2.3, some phase portraits for the averaged equations are presented. In Section 4, some conclusions will be given. Finally, the analytical proofs of Hopf and pitchfork bifurcations are given in Appendix A.

2. Parametric excitation of a nonlinear aeroelastic plunge oscillator

In this section the parametric excitation of a nonlinear aeroelastic plunge oscillator is analyzed. A quasi steady approximation for the aeroelastic force is used. Consequently, the equation of motion is derived. The analysis of this equation is presented, which is based on the averaging method.

2.1. Derivation of the model equation

In Parkinson and Smith (1964), Blevins (1990) and Haaker (1996), the equation of motion for the plunge oscillator is derived as follows:

$$m\ddot{y} + b\dot{y} + ky = \frac{1}{2}\rho dlU^2 C_N(\alpha), \tag{1}$$

where α denotes the so called angle of attack, which in the dynamic situation may be approximated through $\alpha = -\dot{y}/U$.

Here we assume a periodically varying stiffness according to $k = k_0 - k_1\cos(\Omega t)$. We introduce the system parameters ω (frequency), ε (small parameter) and μ (reduced velocity) according to $\omega^2 = k_0/m$, $\varepsilon = \rho d^2 l/(2m)$ and $\mu = U/(\omega d)$. Note that ε may be assumed a small parameter due to air density ρ being of the order 10^{-3}. Defining a new damping coefficient β and parametric excitation coefficient a according to $\beta\varepsilon = b/(2m\omega)$ and $\varepsilon a = k_1/(m\omega^2)$, respectively, and introducing new variables x and τ according to $x = \omega y/U$ and $\tau = \omega t$, respectively then one gets the equation

$$x'' + \left(1 - \varepsilon a\cos\left(\frac{\Omega}{\omega}\tau\right)\right)x = \varepsilon(-2\beta x' + \mu C_N(\alpha)), \tag{2}$$

with $\alpha = -x'$ and the apostrophe denotes the differentiation with respect to τ.

Finally we take for the aerodynamic coefficient curve C_N a cubic polynomial $C_N = c_1\alpha + c_2\alpha^2 + c_3\alpha^3$, with $c_1 < 0, c_3 > 0$ [relevant for cylinders with nearly circular cross section; see for example Nigol and Buchan (1981)].

Then the model equation we obtain is

$$x'' + \left(1 - \varepsilon a\cos\left(\frac{\Omega}{\omega}\tau\right)\right)x = \varepsilon(-(2\beta + c_1\mu)x' + c_2\mu x'^2 - c_3\mu x'^3). \tag{3}$$

This equation is a nonlinear Mathieu equation.

2.2. Analysis of the model equation

In this subsection an amplitude-phase transformation is applied to transform the system (3) to a suitable form for applying the averaging method.

We define amplitude r and phase ψ or alternatively euclidean coordinates u and v through

$$x = r(\tau)\cos(\tau + \psi(\tau)), \tag{4}$$

$$x' = -r(\tau)\sin(\tau + \psi(\tau)), \tag{5}$$

or

$$x = u(\tau)\cos(\tau) + v(\tau)\sin(\tau), \tag{6}$$

$$x' = -u(\tau)\sin(\tau) + v(\tau)\cos(\tau). \tag{7}$$

Note that the following relation between the coordinate pairs holds $u = r\cos(\psi)$ and $v = -r\sin(\psi)$.

To obtain the averaged equations in (r,ψ) or (u,v) coordinates one substitutes expressions (4), (5) or (6), (7) into Eq. (3). To simplify the equations we transform $r\to\bar{r}/\sqrt{c_3}$, or equivalently $(u,v)\to\left(\bar{u}/\sqrt{c_3},\bar{v}/\sqrt{c_3}\right)$. After setting $\Omega/\omega=2+\varepsilon\delta$ with δ a detuning coefficient, and transforming the time $(2+\varepsilon\delta)\tau\to 2s$, then after neglecting the "bar", one obtains the following averaged equations for (r',ψ') and for (u',v'), respectively (the prime denotes $\mathrm{d}/\mathrm{d}s$)

$$r'=\varepsilon\left(-\left(\frac{a}{4}\sin(2\psi)+\beta+\frac{1}{2}c_1\mu\right)r-\frac{3}{8}\mu r^3\right), \tag{8}$$

$$\psi'=\varepsilon\left(-\frac{\delta}{2}-\frac{a}{4}\cos(2\psi)\right) \tag{9}$$

and

$$u'=\varepsilon\left(-\left(\beta+\frac{1}{2}c_1\mu\right)u+\left(\frac{a}{4}-\frac{\delta}{2}\right)v-\frac{3}{8}\mu(uv^2+u^3)\right), \tag{10}$$

$$v'=\varepsilon\left(\left(\frac{\delta}{2}+\frac{a}{4}\right)u-\left(\beta+\frac{1}{2}c_1\mu\right)v-\frac{3}{8}\mu(u^2v+v^3)\right). \tag{11}$$

Note that in this paper we choose $\Omega/\omega=2+\varepsilon\delta$, because the most dangerous situations arise when the frequency of the parametric excitation is close to two times the oscillator frequency, see for example Da Costa et al. (1996) and Verhulst (1996). Before starting the analysis we show that both a and δ may be assumed positive. Suppose a solution of Eqs. (8) and (9) is denoted as $(r(s;a,\delta),\psi(s;a,\delta))$. Then, if in Eqs. (8) and (9) a is replaced by $-a$, it is readily shown that the solution of this new equation follows from the solution of the original equations as follows:

$$(r(s;-a,\delta),\psi(s;-a,\delta))=\left(r(s;a,\delta),\psi(s;a,\delta)+\frac{\pi}{2}\right).$$

Similarly, one may show that

$$(r(s;a,-\delta),\psi(s;a,-\delta))=\left(r(s;a,\delta),-\psi(s;a,\delta)+\frac{\pi}{2}\right).$$

2.2.1. Stability analysis of the trivial solution

From Eqs. (10) and (11), one obtains the eigenvalues evaluated at $(0,0)$ as follows $\lambda_{01}=-\frac{1}{2}c_1\mu-\beta-\frac{1}{4}\sqrt{a^2-4\delta^2}$ and $\lambda_{02}=-\frac{1}{2}c_1\mu-\beta+\frac{1}{4}\sqrt{a^2-4\delta^2}$.

Depending on the strength of the parametric excitation a compared to detuning δ and structural damping β one obtains the following cases.

(i) In the case $2\delta/a<1$, both eigenvalues evaluated at (0,0) are real.

Note that $\lambda_{01}<\lambda_{02}$, so the equilibrium position is stable if $\lambda_{02}<0$. Even without wind, i.e. $\mu=0$, the equilibrium position may be unstable, depending on the sign of $-\beta+\frac{1}{4}\sqrt{a^2-4\delta^2}$, that is,

(a) if $a^2>4\delta^2+16\beta^2$, i.e., if the parametric resonance is strong compared to detuning and damping, then the equilibrium position is a saddle for $\mu=0$; in that case a stable nontrivial critical point (r_2,ψ_2) exists; note that if μ is increased from zero, one finds that for $\mu=-2\beta/c_1-1/(2c_1)\sqrt{a^2-4\delta^2}$, a pitchfork bifurcation occurs in which an unstable critical point (r_1,ψ_1) is born;

(b) if $a^2<4\delta^2+16\beta^2$, then the equilibrium solution is stable for $\mu=0$; on increasing μ from zero a critical flow velocity $\mu=-2\beta/c_1+1/(2c_1)\sqrt{a^2-4\delta^2}$ is reached for which a pitchfork bifurcation occurs in which a stable critical point (r_2,ψ_2) is born; increasing μ further such that $\lambda_{01}=0$, one finds the second pitchfork bifurcation in which an unstable critical point (r_1,ψ_1) is born.

(ii) In the case $2\delta/a=1$, the stability of $(0,0)$ is determined by the sign of $-\frac{1}{2}c_1\mu-\beta$, i.e., a critical flow velocity $\mu_{c_r}=-2\beta/c_1$ exists such that the equilibrium position is unstable for $\mu>\mu_{c_r}$. At $\mu=\mu_{c_r}$ a pitchfork bifurcation occurs indicating the loss of stability of the trivial solution and the creation of a stable nontrivial solution.

(iii) In the case $2\delta/a>1$, both of the eigenvalues are complex. The equilibrium solution is stable if $\mu<\mu_{c_r}$. We see that for $\mu<\mu_{c_r}$, $(0,0)$ is a stable focus. At $\mu=\mu_{c_r}$, the eigenvalues are purely imaginary which indicates that there exists a Hopf bifurcation leading to the creation of a stable limit cycle. This limit cycle corresponds to a solution with periodically modulated amplitudes and phases for the original equation. For $\mu>\mu_{c_r}$, the equilibrium position becomes an unstable focus.

2.2.2. Nonlinear analysis

Note that Eqs. (8) and (9) have the following so called rotational symmetry: $(r,\psi)\to(r,\psi+\pi)$. This indicates that if (r,ψ) is a solution of (8) and (9) then $(r,\psi+\pi)$ is also a solution. In the phase portrait the solution $(r,\psi+\pi)$ is obtained by rotating the solution (r,ψ) over π. In the sequel we only consider $0\leqslant\psi\leqslant\pi$. Setting the right hand side of Eq. (9) to zero, one gets

$$\cos(2\psi)=-\frac{2\delta}{a}. \tag{12}$$

We consider again the three cases by extending the linear analysis.

(i) In the case $2\delta/a<1$ there are two solutions for Eq. (12), say ψ_1 and ψ_2. Assume that $\psi_1<\psi_2$ then $\sin(2\psi_1)>0$ and $\sin(2\psi_2)<0$.

From Eq. (8) one gets that $r=\{-8/(3\mu)(a/4\sin(2\psi)+\beta+\frac{1}{2}c_1\mu)\}^{1/2}$ and $\cos(2\psi)=-2\delta/a$. From here one finds that $\sin(2\psi)=\pm1/a\sqrt{a^2-4\delta^2}$. For $\psi=\psi_1$ then we have $r_1=(8\lambda_{01}/(3\mu))^{1/2}$. The solution (r_1,ψ_1) exists for $\mu>-2\beta/c_1-1/(2c_1)\sqrt{a^2-4\delta^2}$. Its eigenvalues are $\lambda_{11}=\frac{1}{2}\sqrt{a^2-4\delta^2}+2\beta+c_1\mu$ and $\lambda_{12}=\frac{1}{2}\sqrt{a^2-4\delta^2}>0$. We conclude that (r_1,ψ_1) is always unstable.

For $\psi=\psi_2$ then we have $r_2=(8\lambda_{02}/(3\mu))^{1/2}$. The solution (r_2,ψ_2) exists for $\mu>-2\beta/c_1+1/(2c_1)\sqrt{a^2-4\delta^2}$. Its eigenvalues are $\lambda_{21}=-\frac{1}{2}\sqrt{a^2-4\delta^2}+2\beta+c_1\mu$ and $\lambda_{22}=-\frac{1}{2}\sqrt{a^2-4\delta^2}<0$. The eigenvalue $\lambda_{21}<0$ if and only if $\mu>-2\beta/c_1-1/(2c_1)\sqrt{a^2-4\delta^2}$. From here we conclude that the solution (r_2,ψ_2) is always stable.

(ii) In the case $2\delta/a=1$ the solutions of Eq. (12) is $\psi_2=\pi/2$. From Eq. (8) one gets $r=\{8/(3\mu)(-\beta-\frac{1}{2}c_1\mu)\}^{1/2}$. The nontrivial solution is stable and exists for $\mu>\mu_{c_r}$.

(iii) In the case $2\delta/a>1$ there is no nontrivial solution at all. Instead of this one finds a stable limit cycle born in the Hopf bifurcation for $\mu=\mu_{c_r}$.

2.2.3. Phase portraits for the averaged equations

Some phase portraits for the averaged equations for the case $2\delta/a<1$ are given in this subsection. Assume $a=1$, $\beta=0.5$, $c_1=-1$ and $\delta=0.125$. Then one gets that for a wind velocity $\mu=0.4$ there is only one solution, i.e., the trivial solution as a stable node, see Fig. 3(a). For $\mu=0.8$ one gets the trivial solution as a saddle and two symmetric nontrivial solutions as stable nodes, see Fig. 3(b). For $\mu=1.8$ one gets the trivial solution as an unstable node and two pairs of nontrivial solutions, i.e, two stable nodes and two saddles, see Fig. 3(c).

3. Parametric excitation of a nonlinear aeroelastic seesaw oscillator

In this section the parametric excitation of a nonlinear aeroelastic seesaw oscillator is analyzed. Based on the quasi steady approach the equation of motion is derived and using the averaging method the analysis of this equation is presented.

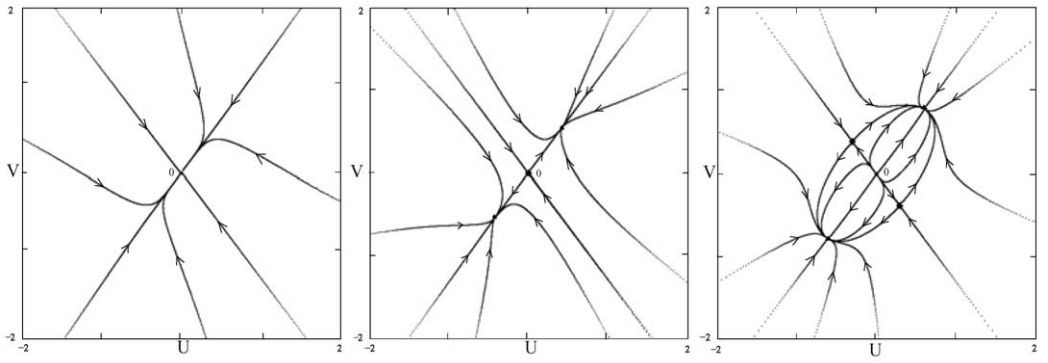

Fig. 3. Phase portraits for $a=1$, $\beta=0.5$, $c_1=-1$, and $\delta=0.125$. (a) $\mu=0.4$, (b) $\mu=0.8$ and (c) $\mu=1.8$.

3.1. Derivation of the model equation

In this paper θ denotes the angle of rotation of the seesaw structure around the hinge axis. Following Haaker (1996) and Haaker and Van Oudheusden (1997), the following equation describes the aeroelastic response of the seesaw oscillator to a homogeneous uniform wind flow

$$I\ddot{\theta} + c\dot{\theta} + m_p gh \sin\theta = \frac{1}{2}\rho dlRU^2 C_N(\alpha). \tag{13}$$

Here I, c, m_p, g and h are the structural moment of inertia, the linear viscous damping coefficient, the pendulum mass, the gravity constant, and the pendulum length, respectively. The right hand side of Eq. (13) represents the external aerodynamic force where ρ, d, l, and R denote air density, a characteristic length of the cross section, the length of the cylinder and the distance from the cylinder's axis to the hinge axis, respectively. Finally, U denotes the wind velocity and α denotes the instantaneous angle of attack.

Assuming periodically varying pendulum length $h = h_0(1 - \frac{1}{2}\tilde{h}\cos(\Omega t))$, one gets

$$I = I_0 - \tilde{h} m_p h_0^2 \cos(\Omega t) + \mathcal{O}(\tilde{h}^2), \tag{14}$$

where I_0 denotes the structural moment of inertia corresponding with fixed pendulum length h_0, $\tilde{h}$ denotes the relative amplitude of the periodic variation which is assumed small. So from equations (13) and (14) one obtains

$$(I_0 - \tilde{h} m_p h_0^2 \cos(\Omega t))\ddot{\theta} + c\dot{\theta} + m_p g h_0 (1 - \tilde{h}\cos(\Omega t)) \sin\theta = \frac{1}{2}\rho dlRU^2 C_N(\alpha) + \mathcal{O}(\tilde{h}^2). \tag{15}$$

Let $v = m_p h_0^2$ and $\sin\theta \approx \theta$, one can rewrite Eq. (15) to become

$$\ddot{\theta} + \frac{c}{I_0}\left(1 + \frac{v\tilde{h}}{I_0}\cos(\Omega t)\right)\dot{\theta} + \frac{m_p g h_0}{I_0}(1 - \tilde{h}\cos(\Omega t))\left(1 + \frac{v\tilde{h}}{I_0}\cos(\Omega t)\right)\theta = \frac{\rho dlR}{2I_0} U^2 C_N(\alpha)\left(1 + \frac{v\tilde{h}}{I_0}\cos(\Omega t)\right). \tag{16}$$

Scaling time with $\tau = \omega t$, where $\omega^2 = m_p g h_0 / I_0$ and introducing $\varepsilon = \rho l d R^3/(2I_0)$; $\mu = U/(\omega R)$; $2\beta\varepsilon = c/(I_0\omega)$ and assuming $\tilde{h} = \tilde{a}\varepsilon$, then one finds

$$\theta'' + \theta = \varepsilon\left(\tilde{a}\left(1 - \frac{v}{I_0}\right)\cos\left(\frac{\Omega}{\omega}\tau\right)\theta - 2\beta\theta' + \mu^2 C_N(\alpha)\right) + \mathcal{O}(\varepsilon^2). \tag{17}$$

Letting $a = \tilde{a}(1 - v/I_0) > 0$, one obtains

$$\theta'' + \left(1 - \varepsilon a \cos\left(\frac{\Omega}{\omega}\tau\right)\right)\theta = \varepsilon(-2\beta\theta' + \mu^2 C_N(\alpha)) + \mathcal{O}(\varepsilon^2), \tag{18}$$

with $\alpha = \theta - \theta'/\mu$, see Haaker (1996) and $C_N(\alpha) = c_1\alpha + c_2\alpha^2 + c_3\alpha^3, c_1 < 0$ and $c_3 > 0$. So, the equation becomes

$$\theta'' + \theta = \varepsilon\left(\left(a\cos\left(\frac{\Omega}{\omega}\tau\right) + c_1\mu^2\right)\theta - (c_1\mu + 2\beta)\theta' + c_2\mu^2\theta^2 + c_2\theta'^2 - 2c_2\mu\theta\theta' + c_3\mu^2\theta^3 - \frac{c_3}{\mu}\theta'^3 - 3c_3\mu\theta^2\theta' + 3c_3\theta\theta'^2\right) + \mathcal{O}(\varepsilon^2). \tag{19}$$

Eq. (19) is a nonlinear Mathieu equation.

3.2. Analysis of the model equation

To reduce complexity in the first order perturbation analysis we set $\Omega/\omega = 2 + \delta$, with $\delta = \mathcal{O}(\varepsilon^2)$ rather than $\delta = \mathcal{O}(\varepsilon)$, and thus remove δ from our first order averaged equations. We define amplitude r and phase ψ or alternatively coordinates u and v through

$$\theta = r(\tau)\cos(\tau + \psi(\tau)), \tag{20}$$

$$\theta' = -r(\tau)\sin(\tau + \psi(\tau)), \tag{21}$$

or

$$\theta = u(\tau)\cos(\tau) + v(\tau)\sin(\tau), \tag{22}$$

$$\theta' = -u(\tau)\sin(\tau) + v(\tau)\cos(\tau). \tag{23}$$

Substituting Eqs. (20)–(23) into (19) one obtains the averaged equations for r and ψ or for u and v, respectively, as follows:

$$r' = \varepsilon\left(\frac{1}{4}(-4\beta - 2c_1\mu + a\sin(2\psi))r - \frac{3c_3}{8\mu}(1+\mu^2)r^3\right), \tag{24}$$

$$\psi' = \varepsilon\left(\frac{a}{4}\cos(2\psi) + \frac{c_1\mu^2}{2} + \frac{3c_3}{8}(1+\mu^2)r^2\right), \tag{25}$$

or

$$u' = \varepsilon\left(-\left(\frac{c_1}{2}\mu+\beta\right)u + \frac{1}{4}(a-2c_1\mu^2)v - \frac{3c_3}{8}\left(\frac{1}{\mu}+\mu\right)uv^2 - \frac{3c_3}{8}(1+\mu^2)u^2v - \frac{3c_3}{8}\left(\frac{1}{\mu}+\mu\right)u^3 - \frac{3c_3}{8}(1+\mu^2)v^3\right), \tag{26}$$

$$v' = \varepsilon\left(+\frac{1}{4}(a+2c_1\mu^2)u - \left(\frac{c_1}{2}\mu+\beta\right)v + \frac{3c_3}{8}(1+\mu^2)uv^2 - \frac{3c_3}{8}\left(\frac{1}{\mu}+\mu\right)u^2v + \frac{3c_3}{8}(1+\mu^2)u^3 - \frac{3c_3}{8}\left(\frac{1}{\mu}+\mu\right)v^3\right). \tag{27}$$

3.2.1. Stability of the trivial solution

For the linear analysis of the trivial solution we use the (u,v)-coordinates, i.e. Eqs. (26) and (27). One can find that $(0,0)$ is a critical point of (26) and (27).

Transforming $u \to \sqrt{4|c_1|\mu/(3c_3(1+\mu^2))}\tilde{u}$, $v \to \sqrt{4|c_1|\mu/(3c_3(1+\mu^2))}\ \tilde{v}$, and time $\tau \to |c_1|s/2$, one finds (after neglecting the 'tilde' and denoting $\mathrm{d}/\mathrm{d}s$ by the overdot)

$$\dot{u} = \varepsilon\left(\left(\mu - \frac{2\beta}{|c_1|}\right)u + \left(\frac{a}{2|c_1|}+\mu^2\right)v - uv^2 - \mu u^2 v - u^3 - \mu v^3\right), \tag{28}$$

$$\dot{v} = \varepsilon\left(\left(\frac{a}{2|c_1|}-\mu^2\right)u + \left(\mu - \frac{2\beta}{|c_1|}\right)v + \mu uv^2 - u^2v + \mu u^3 - v^3\right). \tag{29}$$

Letting $p = 2\beta/|c_1|$ and $q = a/(2|c_1|)$ then one obtains

$$\dot{u} = \varepsilon((\mu - p)u + (\mu^2+q)v - uv^2 - \mu u^2 v - u^3 - \mu v^3), \tag{30}$$

$$\dot{v} = \varepsilon((-\mu^2+q)u + (\mu-p)v + \mu uv^2 - u^2v + \mu u^3 - v^3). \tag{31}$$

The eigenvalues evaluated at the critical point $(0,0)$ are

$$\lambda_1 = (\mu - p) + \sqrt{q^2-\mu^4},$$
$$\lambda_2 = (\mu - p) - \sqrt{q^2-\mu^4}.$$

Note that $\mathscr{R}e(\lambda_1) > \mathscr{R}e(\lambda_2)$ always holds, therefore the stability of the trivial solution is determined by $\mathscr{R}e(\lambda_1) < 0$.

In absence of parametric excitation, i.e. $q = 0$, the stability of the trivial solution is completely determined by the sign of $\mu - p$. If $\mu < p$, the trivial solution is stable; if $\mu > p$ the trivial solution is unstable. In fact $\mu = p = -2\beta/c_1$ is the familiar critical flow velocity corresponding to the Den Hartog's criterion for instability. If $q \neq 0$ and $\mu \geqslant \sqrt{q}$ holds then the trivial solution is stable if $\mu < p$ and unstable if $\mu > p$.

It remains to check what happens if $q \neq 0$ and $\mu < \sqrt{q}$. In that case both eigenvalues are real. Because of that the trivial solution is stable if eigenvalue λ_1 is negative. One gets for $\mu > \sqrt{q}$

$$\frac{\mathrm{d}\lambda_1}{\mathrm{d}\mu} = 1 - \frac{2\mu^3}{\sqrt{q^2-\mu^4}}, \quad \frac{\mathrm{d}^2\lambda_1}{\mathrm{d}\mu^2} = -\left(\frac{6q^2\mu^2 - 2\mu^6}{(q^2-\mu^4)}\frac{1}{\sqrt{q^2-\mu^2}}\right) < 0,$$
$$\frac{\mathrm{d}\lambda_1}{\mathrm{d}\mu}(0) = 1, \quad \lim_{\mu \to \sqrt{q}} \frac{\mathrm{d}\lambda_1}{\mathrm{d}\mu}(\mu) = -\infty, \quad \lambda_1(0) = q - p.$$

From these expressions it follows that λ_1 first increases with increasing μ until a maximum value, say $\lambda_{1_{\max}}$, is reached and then strictly decreases. Because of that λ_1 has at most two roots.

One can distinguish between two main cases as follows: A. Case $p < \sqrt{q}$. B. Case $p > \sqrt{q}$.

In the (q,p) parameter plane, the cases A and B are separated by the curve $p = \sqrt{q}$ as shown in Fig. 4.

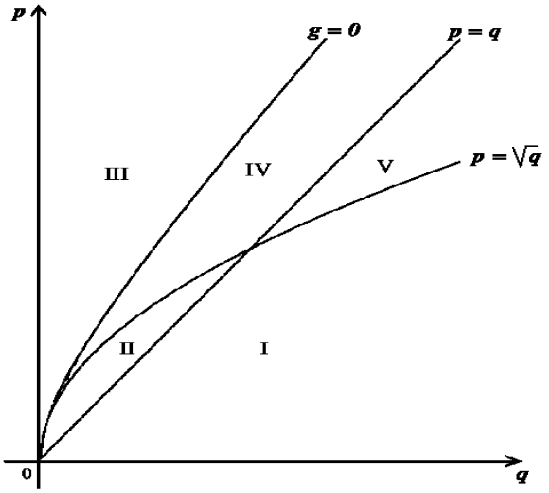

Fig. 4. Diagram of the region in the (q,p) plane.

A. Case $p<\sqrt{q}$.

In this case one finds that $\lambda_1\left(\sqrt{q}\right)=\sqrt{q}-p>0$. The region may be divided into two parts. The region I is the region below of the curves $p=\sqrt{q}$ and $p=q$. The region II is the closed region between the curve $p=\sqrt{q}$ and the line $p=q$, see Fig. 4. In region I, one finds $\lambda_1(0)=q-p>0$. Combined with $\lambda_1\left(\sqrt{q}\right)>0$ and $\mathrm{d}^2\lambda_1/\mathrm{d}\mu^2<0$, it follows that $\lambda_1(\mu)$ is positive for $0<\mu<\sqrt{q}$. Therefore (0, 0) is unstable.

From the properties of $\lambda_2(\mu)$ it follows that a single root μ_2 for λ_2 exists with $\mu_2<\sqrt{q}$. Therefore the trivial solution is a saddle for $\mu<\mu_2$ and an unstable node for $\mu_2<\mu<\sqrt{q}$. Finally, for $\mu>\sqrt{q}$ it follows from the assumption $p<\sqrt{q}$ that the trivial solution is an unstable focus. In region II, one finds $\lambda_1(0)<0$. Combined with $\mathrm{d}\lambda_1/\mathrm{d}\mu(0)>0$, $\mathrm{d}^2\lambda_1/\mathrm{d}\mu^2<0$, and $\lambda_1\left(\sqrt{q}\right)>0$ one finds that a single root μ_1 exists for λ_1 in the interval $0<\mu<\sqrt{q}$. Therefore the trivial solution is stable for $\mu<\mu_1$ and unstable for $\mu_1<\mu<\sqrt{q}$. For $\mu=\mu_1$, a pitchfork bifurcation occurs in which a stable nontrivial solution is born. The type of the instability also depends on the sign of λ_2. From the properties of λ_2 it readily follows that a single root μ_2 for λ_2 exists with $\mu_1<\mu_2<\sqrt{q}$. The trivial solution is a saddle for $\mu_1<\mu<\mu_2$ and an unstable node for $\mu_2<\mu<\sqrt{q}$. Again for $\mu>\sqrt{q}$, the trivial solution is an unstable focus. One gets a stability diagram for the trivial solution in the regions I and II as in Figs. 5(a) and 5(b), respectively.

B. Case $p>\sqrt{q}$.

In this case one finds that $\lambda_1\left(\sqrt{q}\right)=\sqrt{q}-p<0$. Note that $\mathrm{d}\lambda_2/\mathrm{d}\mu=1+2\mu^3/\sqrt{q^2-\mu^4}>0$, $\lambda_2(0)<0$, $\lambda_2(\sqrt{q})<0$. It shows that $\lambda_2(\mu)<0$ for $0<\mu\leqslant\sqrt{q}$.

Above the line $p=q$ one finds $\lambda_1(0)=-p+q<0$. One obtains two roots if $\lambda_{1_{\max}}>0$, no root if $\lambda_{1_{\max}}<0$. The cases are separated by the case $\lambda_{1_{\max}}=0$, i.e., the case for which $\lambda_1(\mu)$ has a double root. Solving $\lambda_1=0$ and $\mathrm{d}\lambda_1/\mathrm{d}\mu=0$ for μ one obtains a curve $g(q,p)=0$ in (q,p)-plane on which a double root occurs, with

$$g(q,p)=-p+\frac{1}{6}k-\frac{1}{k}+\left(q^2-\left(\frac{1}{6}k-\frac{1}{k}\right)^4\right)^{1/2}, \tag{32}$$

where $k=\left(54p+6\sqrt{6+81p^2}\right)^{1/3}$.

Above $g=0$, in the region III, we find $\lambda_{1_{\max}}<0$, and no root exist. The trivial solution is a stable node for $0<\mu<\sqrt{q}$. The stability diagram is shown in 5(c).

Below $g=0$, in region IV, we find $\lambda_{1_{\max}}>0$, and two roots μ_{11} and μ_{12} for λ_1 are found. The trivial solution is a stable node for $0<\mu<\mu_{11}$. It is a saddle for $\mu_{11}<\mu<\mu_{12}$ and again a stable node for $\mu_{12}<\mu<\sqrt{q}$. Furthermore, it is a stable focus for $\sqrt{q}<\mu<p$ and an unstable focus for $\mu>p$. The stability diagram is shown in Fig. 5(d).

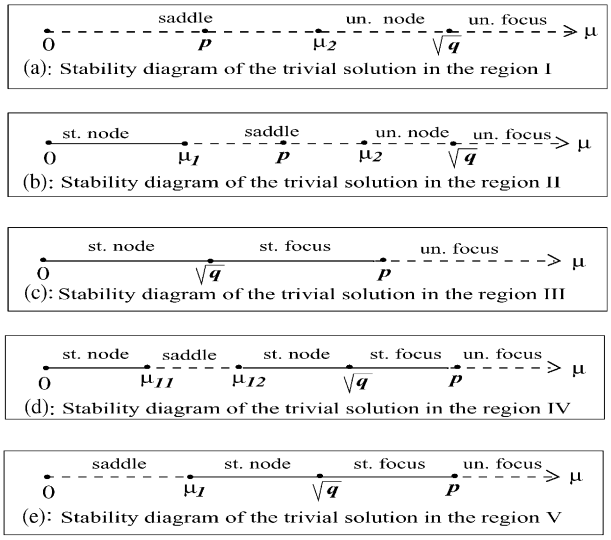

Fig. 5. Diagram of the stability of the trivial solution.

Finally, in region V, between the curves $p = q$ and $p = \sqrt{q}$, one has $\lambda_1(0) = -p + q > 0$. In that case a single root μ_1 for λ_1 exists. Then the trivial solution is a saddle for $0 < \mu \leqslant \mu_1$, a stable node for $\mu_1 < \mu < \sqrt{q}$, stable focus for $\sqrt{q} < \mu < p$, and an unstable focus for $\mu > p$. The stability diagram is shown in Fig. 5(e).

Furthermore one can see that for the case $p > \sqrt{q}$ at $\mu = p$, the system has a purely imaginary pair of eigenvalues. It indicates the occurrence of a Hopf bifurcation. After a straightforward calculation, one gets the Lyapunov number

$$\sigma = -\frac{1}{8}\left(1 - \frac{p^2 + q}{-p^2 + q}\right) < 0. \tag{33}$$

See Appendix A.1 for a proof. This Hopf bifurcation therefore indicates the creation of a stable limit cycle in the averaging equations. This corresponds to oscillations in the original system with periodically modulated amplitudes and phases.

We finally remark that the zeroes of the eigenvalues λ_1 and λ_2 are related to pitchfork bifurcations which involve the creation of branches of nontrivial critical points. See Appendix A.2 for a proof.

3.2.2. Nonlinear analysis

In the analysis of the nontrivial solutions, the averaged equations in polar coordinates are used. Transforming Eqs. (30) and (31) into polar coordinates by using $u = r\cos(\psi)$ and $v = -r\sin(\psi)$ one gets

$$\dot{r} = \varepsilon((\mu - p - q\sin(2\psi))r - r^3), \tag{34}$$

$$\dot{\psi} = \varepsilon(\mu^2 - q\cos(2\psi) - \mu r^2). \tag{35}$$

Multiplying Eq. (34) by r and setting $R = r^2$ yields

$$\dot{R} = \varepsilon(2(\mu - p - q\sin(2\psi))R - 2R^2), \tag{36}$$

$$\dot{\psi} = \varepsilon(\mu^2 - q\cos(2\psi) - \mu R). \tag{37}$$

Setting the right hand sides of Eqs. (36) and (37) to zero one obtains

$$AR^2 + BR + C = 0, \quad R > 0 \tag{38}$$

with

$$A = 1 + \mu^2,$$
$$B = -2(\mu - p + \mu^3),$$
$$C = \mu^4 - q^2 + (\mu - p)^2.$$

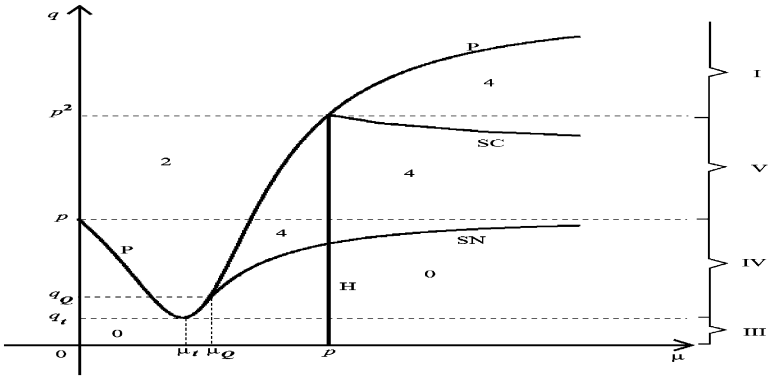

Fig. 6. Number of nontrivial solutions, Hopf (H), saddle connection (SC), saddle-node (SN), and pitchfork (P) bifurcations for case $p > 1$.

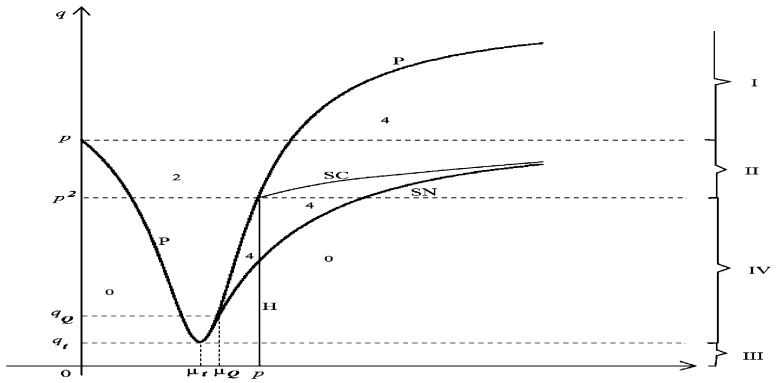

Fig. 7. Number of nontrivial solutions, Hopf (H), saddle connection (SC), saddle-node (SN), and pitchfork (P) bifurcations for case $p < 1$.

The zeroes of Eq. (38) are

$$R_{1,2} = \frac{-B \pm \sqrt{B^2 - 4AC}}{2A}.$$

Note that every solution of Eq. (38) corresponds to two solutions, (R_0, ψ_0) and $(R_0, \psi_0 + \pi)$, of Eqs. (36) and (37). Let D denote the discriminant of (38), then $D = 4((1+\mu^2)q^2 - \mu^2 p^2)$. One gets two positive zeroes of (38) if $C > 0$, $B < 0$, and $D > 0$, one positive zero if $C < 0$, a double positive zero if $D = 0$ and $B < 0$, no positive zero in other cases.

Note that a pitchfork bifurcation occurs for $C = 0$, a saddle-node bifurcation occurs for $D = 0$. Figs. 6 and 7 show the location of saddle-node bifurcation (SN), pitchfork bifurcation (P), Hopf bifurcation (H) and saddle-connection bifurcation (SC) in the (μ, q)-plane for $p > 1$ and $p < 1$, respectively. The saddle-node and pitchfork bifurcation curves have an intersection point Q, in which one gets $B = C = D = 0$. The coordinates of Q are (μ_Q, q_Q), with $\mu_Q = \frac{1}{6}k - 2/k$, $q_Q = \left(\sqrt{6}/6\right)\left(\frac{p}{k}(-k^2 + 6pk + 12)\right)^{1/2}$, and $k = \left(108p + 12\sqrt{12 + 81p^2}\right)^{1/3}$. The equations for the pitchfork bifurcation curve (P) and the saddle-node bifurcation curve (SN) are

$$q_p = (\mu^4 + (\mu - p)^2)^{1/2} \quad \text{and} \quad q_{sn} = \frac{p\mu}{\sqrt{1+\mu^2}},$$

respectively. The coordinate of the minimum point of the pitchfork bifurcation curve is (μ_t, q_t) with $\mu_t = 1/6t - 1/t$, $q_t = (\mu_t^4 + (\mu_t - p)^2)^{1/2}$, and $t = \left(54p + 6\sqrt{6 + 81p^2}\right)^{1/3}$. The Hopf bifurcation is found for $\mu = p$ and $q < p^2$. In Figs. 6 and 7, the numbers denote the number of nontrivial critical point of Eqs. (36) and (37) found in each region. The roman numerals to the right correspond with the stability regions of the linear analysis. Note that $Q = (\mu_Q, q_Q)$ may be viewed

as an 'organizing center' in the parameter plane in the sense that different dynamical behavior can be found in a neighborhood of this point. The pitchfork and the saddle-node bifurcation curves divide the (μ, q)-parameter plane into three big regions, i.e.,

(a) the region where one finds no nontrivial solution;
(b) the region where one finds two nontrivial solutions;
(c) the region where one finds four nontrivial solutions.

The number of nontrivial solutions in each region is determined from the number of positive roots of Eq. (38) in that region.

We now consider Fig. 6, i.e. the case $p > 1$. For a fixed value of $q = q_0$ such that $q_0 > p^2$, starting with a small value of μ, one finds readily two stable nontrivial critical points. Increasing the value of μ such that the pitchfork curve is reached then one gets a pitchfork bifurcation which leads to the creation of two new nontrivial critical points. Two of them are stable foci and the others are saddles. At the point (p, p^2), on the pitchfork curve, one finds that both of the eigenvalues of the trivial solution are zero. From this point, the Hopf (H) and the saddle connection (SC) bifurcation curves start.

For $q = q_0$ such that $p < q_0 < p^2$, starting with a small value of μ, one finds two stable nontrivial critical points. Increasing the value of μ such that the pitchfork curve is reached one obtains another two nontrivial critical points (unstable). At $\mu = p$, a Hopf bifurcation occurs and a stable limit cycle is born. Increasing the value of μ further such that the SC curve is reached the limit cycle disappears in the saddle connection bifurcation (SC). The four nontrivial solutions survive though.

For $q = q_0$ such that $q_Q < q_0 < p$ starting with a small value of μ, one gets only a stable trivial solution. Increasing the value of μ such that the pitchfork bifurcation curve is passed, one finds two stable nontrivial critical points and the trivial solution becomes unstable. Increasing again the value of μ such that the pitchfork bifurcation curve is passed once more, another two unstable critical points are born. However the trivial solution is now stable again. Increasing the value of μ such that the Hopf bifurcation curve is passed one gets a stable limit cycle and four nontrivial solutions. The critical solution is now unstable focus. After increasing the value of μ passed the saddle-node bifurcation curve (SN), both pairs of nontrivial solutions disappear in a saddle-node bifurcation and only the stable limit cycle survives. But if one reaches the saddle-node bifurcation curve (SN) first, then after passing the saddle-node bifurcation curve (SN) both pairs of nontrivial solutions disappear in the saddle-node bifurcation. Finally, increasing the value of μ one gets a stable limit cycle after passing the Hopf bifurcation curve and the trivial solution is an unstable focus.

For $q = q_0$ such that $q_t < q_0 < q_Q$, starting with a small value for μ, then one gets only a stable trivial solution. Increasing the value of μ such that the first pitchfork point is reached then one finds one pair of stable critical points bearing from the pitchfork bifurcation and the trivial solution becomes unstable. Increasing again the value of μ, such that the second pitchfork point is reached then one obtains that the nontrivial critical points disappear and the trivial solution becomes stable. Furthermore, increasing the value of μ, then one obtains a Hopf bifurcation from which the stable limit cycle is born and the trivial solution becomes an unstable focus.

For $q = q_0$ such that $q_0 < q_t$, starting with a small value for μ, then one gets a stable trivial solution. Increasing the value of μ, one gets a Hopf bifurcation from which the stable limit cycle is born and the trivial solution becomes an unstable focus.

The story for Fig. 7 is nearly the same as for Fig. 6. The difference is the saddle connection (SC) bifurcation in Fig. 7, that now corresponds with the creation of a stable limit cycle.

To consider the stability of the nontrivial critical points, one can determine the eigenvalues of the Jacobian from Eqs. (36) and (37) evaluated at (r_0, ψ_0), where $r_0 = \sqrt{R}$ and ψ_0 are determined from the zeroes of Eqs. (36) and (37).

3.2.3. *Phase portraits for the averaged equations*

In this section some phase portraits for the averaged equations (30) and (31) are given. Some special values for the parameters are considered to depict the behaviour of the trivial and the nontrivial solutions in the (u, v)-plane. Depending on the wind velocity μ, one finds how the stability of the trivial solution changes and how the nontrivial critical points and a stable limit cycle appear.

Assuming $p = 2$ and choosing $q = 3.333$ then $p < q < p^2$, one is in the region V, see Fig. 4. The stability diagram of the trivial solution is shown in Fig. 5(e), with $\mu_1 = 1.8243821$ and $\sqrt{q} = 1.82565056$. The bifurcation diagram is depicted in region V of Fig. 6. Varying the value of wind velocity μ one gets following: At $\mu = 1.7$, one finds two nontrivial critical points as stable foci and the trivial critical point as a saddle. The phase portrait in the (u, v)-plane is shown in the Fig. 8(a). Increasing the value of μ such that at $\mu = 1.9$ one obtains two pairs of nontrivial critical points, one pair as saddles and the other pair as stable foci. The trivial solution is a stable focus. The phase portrait is shown in Fig. 8(b). Increasing the value of μ such that $\mu = 2.1$ then one gets two pairs of critical points, one pair as saddles and the other pair as stable foci. The trivial solution is an unstable focus. There is also a stable limit cycle bearing from the Hopf

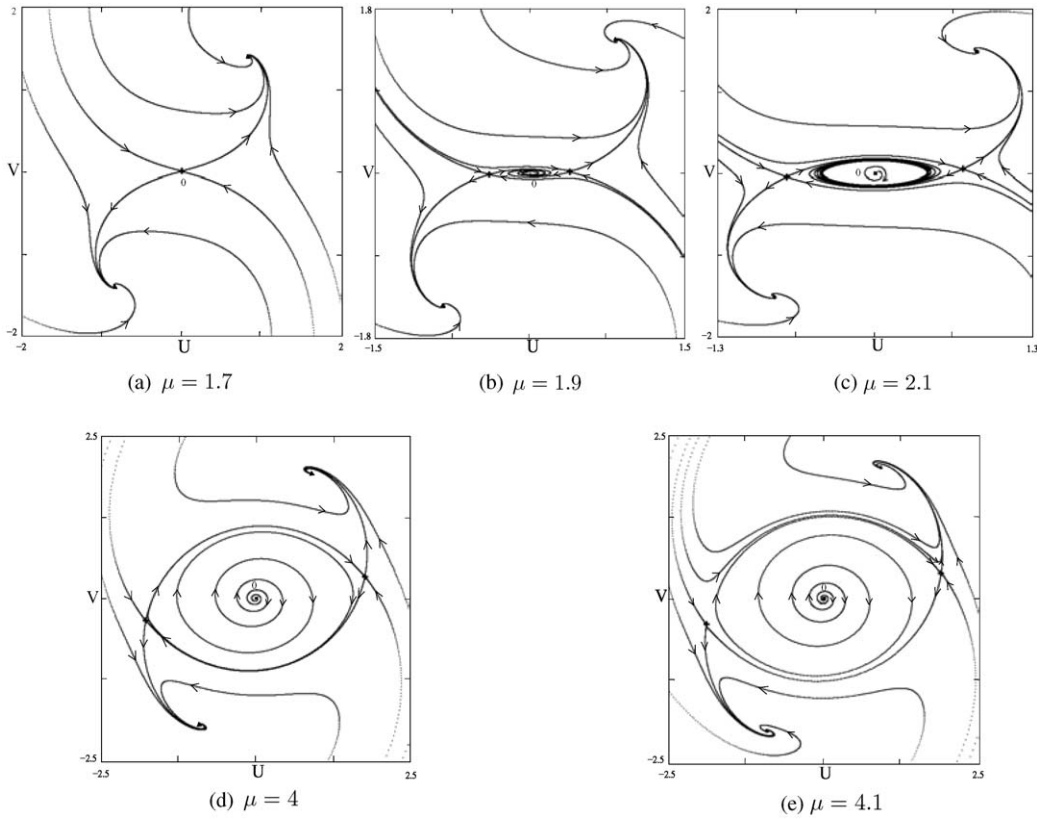

Fig. 8. Phase portraits in the region V for $p = 2$ and $q = 3.333$. (a) $\mu = 1.7$, (b) $\mu = 1.9$, (c) $\mu = 2.1$, (d) $\mu = 4$ and (e) $\mu = 4.1$.

bifurcation at $\mu = p = 2$. The limit cycle corresponds to oscillations in the original system with periodically modulated amplitudes and phases. The phase portrait is shown in Fig. 8(c). For $\mu = 4$ one finds that the limit cycle has disappeared in a heteroclinic loop connecting the two symmetric saddle points, when passing the saddle connection curve. The phase portrait is shown in Fig. 8(d). Finally, for $\mu = 4.1$ one obtains that the saddle connection is broken. All solutions tend to one of the stable foci. The phase portrait is shown in Fig. 8(e).

Assuming $p = 0.5$ and choosing $q = 0.26$ then $p^2 < q < p$ and one is in region II, see Fig. 4. The stability diagram of the trivial solution is shown in Fig. 5(b), with $\mu_1 = 0.2472944$, $\mu_2 = 0.5097236$, and $\sqrt{q} = 0.5099020$. The bifurcation diagram is depicted in region II of Fig. 7. Varying the value of wind velocity μ one gets the behaviour of the solutions as follows: Fig. 9(a) depicts the phase portrait for $\mu = 0.1$. It shows the trivial solution as a stable node, and no other critical points exist.

Increasing the value of μ such that $\mu = \mu_1$ then one of the eigenvalues of the trivial solution is zero. At this point the pitchfork bifurcation occurs which leads to the exchange of stability of the trivial solution. The trivial solution changes from a stable node to a saddle, and the first pair of nontrivial solutions is branched off. These are stable nodes.

At $\mu = 0.4$ one gets a pair of nontrivial solutions as stable nodes and the zero solution as a saddle. The phase portrait in (u, v)-plane as in the Fig. 9(b). Increasing the value of μ such that $\mu = \mu_2$ the second pitchfork bifurcation occurs where the trivial solution changes from a saddle to an unstable node, and a second pair of nontrivial solutions is branched off. These are saddles.

Increasing the value of μ further such that $\mu = 0.57$ then one gets the zero solution is an unstable focus. The phase portrait in (u, v)-plane is as in Fig. 9(c). Increasing again the value of μ such that $\mu = 0.6084$ then one gets a stable limit cycle bearing from the saddle connection bifurcation. Domains of attraction are separated by the stable manifolds of the two saddles. Inside those manifolds the flow tends to the limit cycle, outside it tends to one of the stable node. The phase portrait in the (u, v)-plane is shown in Fig. 9(d). Increasing the value of μ further such that $\mu = 0.8$, one finds saddle-node bifurcations in which the stable and unstable nontrivial solutions disappear. Only the stable limit cycle survives and all flow tends to this limit cycle, see Fig. 9(e).

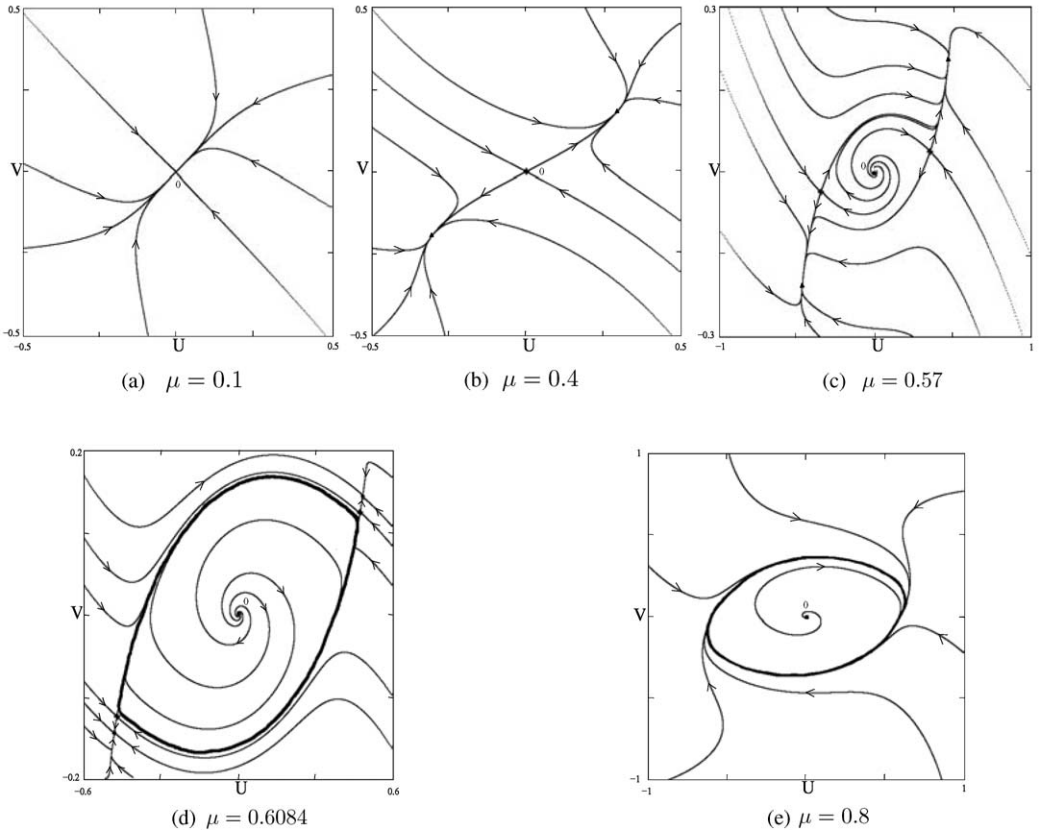

Fig. 9. Phase portraits in the region II for $p = 0.5$ and $q = 0.26$. (a) $\mu = 0.1$, (b) $\mu = 0.4$, (c) $\mu = 0.57$, (d) $\mu = 0.6084$ and (e) $\mu = 0.8$.

4. Conclusions

In this paper the parametric excitation of two nonlinear aeroelastic oscillators was studied. In practice, parametric excitation of structural elements, like bridge stay cables, may be caused by the periodic motion of the bridge deck or the bridge tower. The induced vibrations are most prominent if the excitation frequency is nearly twice the natural frequency.

For the plunge oscillator the following results were obtained:

(i) For strong parametric excitation, i.e. when the ratio of detuning δ and parametric force coefficient a is small, the critical flow velocity is shifted to a lower value. For flow velocities above this value stable periodic oscillations were found. If there is little structural damping, the critical flow velocity shifts to zero, indicating that even in absence of wind the equilibrium position is unstable.

(ii) For weak parametric excitation, $\delta/(2a) > 1$, the well-known critical wind velocity according to Den Hartog's criterion was found. Rather than a stable periodic oscillation, one obtains a stable solution with periodically modulated amplitude and phase.

For the seesaw oscillator the following results were obtained:

(i) The observed behaviour for strong and weak parametric excitation is identical to the behaviour observed for the plunge oscillator.

(ii) Interesting new dynamics is found when the parametric excitation, the structural damping and the linear aeroelastic force are some what balanced. In that case a critical flow velocity may still exist, above which the equilibrium position becomes unstable. However, in some cases the trivial solution re-stabilizes when the flow velocity is increased above a certain value. This may be understood from the fact that the flow velocity causes an increased detuning between the excitation frequency and the natural frequency, which effectively reduces the parametric excitation. Increasing the flow velocity further though, an aeroelastic instability is found for a flow velocity corresponding to Den Hartog's criterion. Next to periodic oscillations also stable periodically modulated solutions are found bearing from limit cycles

in the averaged equations. Both Hopf and saddle connection bifurcations were found responsible for the appearance of these limit cycles. In some cases constant amplitude periodic solutions and periodically modulated solutions were found to co-exist.

Acknowledgements

This research project was sponsored by the Secondary Teacher Development Project (PGSM), Indonesia, with contract No. 6519/0300/Kont-Fel/PGSM and Delft University of Technology, Delft, The Netherlands. The first author is on leave from Jurusan Pendidikan Matematika, FKIP, Universitas Cenderawasih, Jayapura, Papua, Indonesia.

Appendix A

In this appendix the existence of the Hopf and pitchfork bifurcations from the seesaw oscillator are considered.

A.1. The Hopf bifurcation

Consider the system below

$$\dot{u} = \varepsilon((\mu - p)u + (\mu^2 + q)v - uv^2 - \mu u^2 v - u^3 - \mu v^3), \tag{A.1}$$

$$\dot{v} = \varepsilon((-\mu^2 + q)u + (\mu - p)v + \mu uv^2 - u^2 v + \mu u^3 - v^3). \tag{A.2}$$

Letting

$$\mathbf{X} = \begin{pmatrix} u \\ v \end{pmatrix}, \quad \mathbf{A} = \begin{pmatrix} \mu - p & \mu^2 + q \\ -\mu^2 + q & \mu - p \end{pmatrix}, \quad \text{and} \quad \mathbf{F} = \begin{pmatrix} f_1(\mu, u, v) \\ f_2(\mu, u, v) \end{pmatrix},$$

with

$$f_1(\mu, u, v) = -uv^2 - \mu u^2 v - u^3 - \mu v^3,$$
$$f_2(\mu, u, v) = \mu uv^2 - u^2 v + \mu u^3 - v^3,$$

then we have

$$\dot{\mathbf{X}} = \varepsilon(\mathbf{AX} + \mathbf{F}). \tag{A.3}$$

We now transform Eq. (A.3) into a normal form with

$$\mathbf{X} = \mathbf{TZ}, \tag{A.4}$$

where

$$\mathbf{T} = \begin{pmatrix} 0 & a_\mu \\ 1 & 0 \end{pmatrix}, \qquad \mathbf{Z} = \begin{pmatrix} z_1 \\ z_2 \end{pmatrix}$$

and $a_\mu = \sqrt{-(\mu^2 + q)/(-\mu^2 + q)}$; hence we get

$$\mathbf{T}^{-1} = \begin{pmatrix} 0 & 1 \\ \dfrac{1}{a_\mu} & 0 \end{pmatrix}.$$

From Eq. (A.4) we get $u = a_\mu z_2$ and $v = z_1$. So from (A.3) and (A.4) we get

$$\dot{\mathbf{Z}} = \varepsilon((\mathbf{T}^{-1}\mathbf{AT})\mathbf{Z} + \mathbf{G}), \tag{A.5}$$

with

$$\mathbf{G} \equiv \mathbf{T}^{-1}\mathbf{F} = \begin{pmatrix} g_1(\mu, z_1, z_2) \\ g_2(\mu, z_1, z_2) \end{pmatrix},$$

$$\mathbf{T}^{-1}\mathbf{A}\mathbf{T} = \begin{pmatrix} \mu - p & -\dfrac{\mu^2+q}{a_\mu} \\ \dfrac{\mu^2+q}{a_\mu} & \mu - p \end{pmatrix},$$

$$g_1(\mu, z_1, z_2) = \mu a_\mu z_1^2 z_2 - a_\mu z_1 z_2^2 + \mu a_\mu^3 z_2^3 - z_1^3, \tag{A.6}$$

$$g_2(\mu, z_1, z_2) = \frac{1}{a_\mu}(-a_\mu z_1^2 z_2 - \mu a_\mu^2 z_1 z_2^2 - a_\mu^3 z_2^3 - \mu z_1^3). \tag{A.7}$$

At $\mu = p$ we get

$$\begin{pmatrix} \dot{z}_1 \\ \dot{z}_2 \end{pmatrix} = \varepsilon\left(\begin{pmatrix} 0 & -\omega \\ \omega & 0 \end{pmatrix}\begin{pmatrix} z_1 \\ z_2 \end{pmatrix} + \begin{pmatrix} g_1(p, z_1, z_2) \\ g_2(p, z_1, z_2) \end{pmatrix}\right), \tag{A.8}$$

with $\omega = (p^2+q)/a_p >$ and $a_p = \sqrt{(-(p^2+q))/(-p^2+q)} > 0$. In this case we have a pair of purely imaginary eigenvalues of Eq. (A.8).

From Eqs. (A.6) and (A.7) we get $g_{1_{z_1\bar{z}_1 z_1\bar{z}_1}} = -1$, $g_{1_{z_1\bar{z}_2 z_2\bar{z}_2}} = -a_p^2$, $g_{1_{z_1\bar{z}_1}} = 2pa_p z_2 - 6z_1$, $g_{1_{z_1\bar{z}_2}} = 2pa_P z_1 - 2a_p^2 z_2$, $g_{1_{z_2\bar{z}_2}} = -2a_p^2 z_1 + 6pa_p^3 z_2$, $g_{2_{z_2\bar{z}_2 z_2\bar{z}_2}} = -a_p^2$, $g_{2_{z_1\bar{z}_1 z_1\bar{z}_2}} = -1$, $g_{2_{z_1\bar{z}_1}} = -2z_2 - 6\frac{p}{a_p}z_1$, $g_{2_{z_1\bar{z}_2}} = -2z_1 - 2pa_p z_2$ and $g_{2_{z_2\bar{z}_2}} = -2pa_p z_1 - 6a_p^3 z_2$. The Lyapunov number evaluated at (0, 0) is

$$\begin{aligned} \sigma &= \frac{1}{16}(g^1_{z_1 z_1 z_1} + g^1_{z_1 z_2 z_2} + g^2_{z_2 z_2 z_2} + g^2_{z_1 z_1 z_2}) + \frac{1}{16\omega}(g_{1_{z_1\bar{z}_2}}(g_{1_{z_1\bar{z}_1}} + g_{1_{z_2\bar{z}_2}}) - g_{2_{z_1\bar{z}_2}}(g_{2_{z_1\bar{z}_1}} + g_{2_{z_2\bar{z}_2}}) - g_{1_{z_1\bar{z}_1}} g_{2_{z_1\bar{z}_1}} + g_{1_{z_2\bar{z}_2}} g_{2_{z_2\bar{z}_2}}), \\ &= -\frac{1}{8}(1 + a_p^2), \\ &< 0. \end{aligned} \tag{A.9}$$

Using the method in Wiggins (1990, p. 277), we conclude that there is a stable limit cycle bifurcating for $\mu = p$.

A.2. The pitchfork bifurcation

We consider system (A.3), i.e.

$$\dot{\mathbf{X}} = \varepsilon(\mathbf{A}\mathbf{X} + \mathbf{F}). \tag{A.10}$$

The eigenvalues of A are

$$\lambda_1 = \mu - p + \sqrt{-\mu^4 + q^2} \quad \text{and} \quad \lambda_2 = \mu - p - \sqrt{-\mu^4 + q^2}.$$

Let

$$\mathbf{T} = \begin{pmatrix} -b_\mu & b_\mu \\ 1 & 1 \end{pmatrix} \quad \text{then } \mathbf{T}^{-1} = \frac{1}{2}\begin{pmatrix} -\dfrac{1}{b_\mu} & 1 \\ \dfrac{1}{b_\mu} & 1 \end{pmatrix} \quad \text{and} \quad \mathbf{T}^{-1}\mathbf{A}\mathbf{T} = \begin{pmatrix} \mu - p + \sqrt{-\mu^4 + q^2} & 0 \\ 0 & \mu - p - \sqrt{-\mu^4 + q^2} \end{pmatrix},$$

with $b_\mu = \sqrt{-\mu^4 + q^2}/(\mu^2 - q)$. We transform Eq. (A.10) with

$$\mathbf{X} = \mathbf{T}\mathbf{Z}, \tag{A.11}$$

where

$$\mathbf{Z} = \begin{pmatrix} z_1 \\ z_2 \end{pmatrix}.$$

Then we get $u = b_\mu(-z_1 + z_2)$, $v = z_1 + z_2$ and

$$\begin{aligned} f_1(\mu, z_1, z_2) &= a_{30} z_1^3 + a_{21} z_1^2 z_2 + a_{12} z_1 z_2^2 + a_{03} z_2^2, \\ f_2(\mu, z_1, z_2) &= b_{30} z_1^3 + b_{21} z_1^2 z_2 + b_{12} z_1 z_2^2 + b_{03} z_2^2, \end{aligned}$$

where

$$a_{30} = b_\mu - \mu b_\mu^2 + b_\mu^3 - \mu, \quad a_{21} = b_\mu + \mu b_\mu^3 - 3b_\mu^3 - 3\mu,$$
$$a_{12} = -b_\mu + \mu b_\mu^2 - 3b_\mu^2 - 3\mu, \quad a_{03} = -(b_\mu + \mu b_\mu^2 + b_\mu^3 + \mu) < 0,$$
$$b_{30} = -(\mu b_\mu + b_\mu^2 + \mu b_\mu^3 + 1) < 0, \quad b_{21} = -\mu b_\mu + b_\mu^2 + 3\mu b_\mu^3 - 3,$$
$$b_{12} = \mu b_\mu + b_\mu^2 - 3\mu b_\mu^3 - 3, \quad b_{03} = \mu b_\mu - b_\mu^2 + \mu b_\mu^3 - 1.$$

Consider that

$$\begin{aligned}\dot{\mathbf{Z}} &= \varepsilon((\mathbf{T}^{-1}\mathbf{A}\mathbf{T})\mathbf{Z} + \mathbf{T}^{-1}\mathbf{F}),\\ &= \varepsilon\left(\begin{pmatrix} \mu - p + \sqrt{-\mu^4 + q^2} & 0 \\ 0 & \mu - p - \sqrt{-\mu^4 + q^2} \end{pmatrix}\begin{pmatrix} z_1 \\ z_2 \end{pmatrix} + \begin{pmatrix} h_1(\mu, z_1, z_2) \\ h_2(\mu, z_1, z_2) \end{pmatrix}\right),\end{aligned} \tag{A.12}$$

where

$$h_1(\mu, z_1, z_2) = \alpha_{30} z_1^3 + \alpha_{21} z_1^2 z_2 + \alpha_{12} z_1 z_2^2 + \alpha_{03} z_2^3, \tag{A.13}$$

$$h_2(\mu, z_1, z_2) = \beta_{30} z_1^3 + \beta_{21} z_1^2 z_2 + \beta_{12} z_1 z_2^2 + \beta_{03} z_2^3, \tag{A.14}$$

with $\alpha_{30} = \frac{1}{2}(b_{30} - a_{30}/b_\mu)$, $\alpha_{21} = \frac{1}{2}(b_{21} - a_{21}/b_\mu)$, $\alpha_{12} = \frac{1}{2}(b_{12} - a_{12}/b_\mu)$, $\alpha_{03} = \frac{1}{2}(b_{03} - a_{03}/b_\mu)$, $\beta_{30} = \frac{1}{2}(a_{30}/b_\mu + b_{30})$, $\beta_{21} = \frac{1}{2}(a_{21}/b_\mu + b_{21})$, $\beta_{12} = \frac{1}{2}(a_{12}/b_\mu + b_{12})$, and $\beta_{03} = \frac{1}{2}(a_{03}/b_\mu + b_{03})$.

From Eq. (A.12), $\lambda_1 = 0$ if $\mu - p = -\sqrt{-\mu^4 + q^2}$. We now consider the pitchfork bifurcation at $\mu = \mu_{\lambda_1}$, i.e. the zero of eigenvalue λ_1. We apply the center manifold theory to our system, i.e. to Eq. (A.12), see Wiggins (1990) and Verhulst (1996). Letting

$$z_2 \equiv h(z_1) = \alpha z_1^2 + \beta z_1^3 + \mathcal{O}(4), \tag{A.15}$$

$$\frac{\mathrm{d}h}{\mathrm{d}z_1} = 2\alpha z_1 + 3\beta z_1^2 + \mathcal{O}(3). \tag{A.16}$$

At $\mu = \mu_{\lambda_1}$ we get

$$a_4 z_1^4 + \mathcal{O}(5) \equiv \eta_2 z_1^2 + \eta_3 z_1^3 + \mathcal{O}(4), \tag{A.17}$$

with

$$a_4 = \alpha\left(b_{30} - \frac{a_{30}}{b_\mu}\right),$$
$$\eta_2 = \alpha\left(\mu - p - \sqrt{-\mu^4 + q^2}\right),$$
$$\eta_3 = \left(\mu - p - \sqrt{-\mu^4 + q^2}\right)\left(\beta + \frac{1}{2}\left(\frac{a_{30}}{b_\mu} + b_{30}\right)\right),$$

After equating the coefficients of (A.17), we get $\alpha = 0$ and $\beta = -\frac{1}{2}(a_{30}/b_\mu + b_{30})$; therefore

$$h(z_1) = \beta z_1^3 + \mathcal{O}(4).$$

The flow in the center manifold at $\mu = \mu_{\lambda_1}$ is determined by the 1-dimensional system as follows:

$$\begin{aligned}\dot{w} &= g_1(\mu, w, h(w)),\\ &= \frac{1}{2}\left(b_{30} - \frac{a_{30}}{2b_\mu}\right)w^3 + \mathcal{O}(5),\end{aligned} \tag{A.18}$$

where $a_{30}/(2b_\mu) = -\left(\mu(\mu^2 - q) - \sqrt{-\mu^4 + q^2}\right)q/\left((\mu^2 - q)\sqrt{-\mu^4 + q^2}\right) > 0$.

Using the theorem (13.4) in Verhulst (1996), we conclude that $(0, 0)$ is stable for $\mu = \mu_{\lambda_1}$.

In the center manifold, the flow is determined by

$$\dot{w} = \left(\mu - p + \sqrt{-\mu^4 + q^2}\right)w + \frac{1}{2}\left(b_{30} - \frac{a_{30}}{2b_\mu}\right)w^3. \tag{A.19}$$

Transforming the time $t \to 2b_\mu/(a_{30} - b_\mu b_{30})\tau$ then Eq. (A.19) becomes

$$w' = \frac{2b_\mu}{a_{30} - b_\mu b_{30}}\left(\mu - p + \sqrt{-\mu^4 + q^2}\right)w - w^3, \tag{A.20}$$

where the prime denotes the differentiation with respect to τ.

Letting $s(\mu) = (2b_\mu/(a_{30} - b_\mu b_{30}))\left(\mu - p + \sqrt{-\mu^4 + q^2}\right)$, we can rewrite (A.20) to become

$$w' = s(\mu)w - w^3 \tag{A.21}$$

We can see that if $s(\mu) \leqslant 0$ then $\lambda_1 \leqslant 0$. In this case there is one equilibrium solution, i.e. $w = 0$ which is stable. If $s(\mu) > 0$ then $\lambda_1 > 0$. In this case there are three solutions, i.e. two stable nontrivial solutions which is branch off at $\mu = \mu_{\lambda_1}$ and an unstable trivial solution. We conclude from Eq. (A.21) that the pitchfork bifurcation exists at $\mu = \mu_{\lambda_1}$.

References

Blevins, R.D., 1990. Flow Induced Vibration, 2nd Edition. Van Nostrand Reinhold, New York.

Da Costa, A.P., Martins, J., Branco, F., Lilien, J.L., 1996. Oscillations of bridge stay cables induced by periodic motions of deck and/or towers. ASCE Journal of Engineering Mechanics 122, 613–622.

Haaker, T.I., 1996. Quasi-steady modelling and asymptotic analysis of aeroelastic oscillators. Ph.D. Thesis, Department of Applied Analysis, Delft University of Technology, The Netherlands.

Haaker, T.I., Van der Burgh, A.H.P., 1994. On the dynamics of aeroelastic oscillators with one degree of freedom. SIAM Journal of Applied Mathematics 54, 1033–1047.

Haaker, T.I., Van Oudheusden, B.W., 1997. One-degree-of-freedom rotational galloping under strong wind conditions. International Journal of Non-Linear Mechanics 32, 803–814.

Lumbantobing, H., Haaker, T.I., 2000. Aeroelastic oscillations of a single seesaw oscillator under strong wind conditions. Journal of Indonesian Mathematical Society 6, 439–444.

Lumbantobing, H., Haaker, T.I., 2002a. Aeroelastic oscillations of a seesaw-type oscillator under strong wind conditions. Journal of Sound and Vibration 257, 439–456.

Lumbantobing, H., Haaker, T.I., 2002b. On the parametric excitation of a nonlinear aeroelastic oscillator. Proceedings of ASME International Mechanical Engineering Congress and Exposition 2002 (IMECE2002), New Orleans, USA, with number: IMECE2002-32163.

Nigol, O., Buchan, P.G., 1981. Conductor galloping part I—Den Hartog mechanism. IEEE Transactions on Power Apparatus and System PAS-100 (2), 699–707.

Parkinson, G.V., Smith, J.D., 1964. The square prism as an aeroelastic non-linear oscillator. Quarterly Journal of Mechanics and Applied Mathematics XVII, 225–239.

Tondl, A., Verhulst, F., Nabergoj, R., 2000. Autoparametric Resonance in Mechanical Systems. Cambridge University Press, Cambridge, NY, USA.

Van der Burgh, A.H.P., 1996. Parametric excitation in mechanical systems. Proceedings of the International Conference on Differential Equations, Theory, Numerics and Applications, Indonesia, pp. 3–16.

Van Oudheusden, B.W., 1996. Rotational one-degree-of-freedom galloping in the presence of viscous and frictional damping. Journal of Fluids and Structures 10, 673–689.

Verhulst, F., 1996. Nonlinear Differential Equations and Dynamical Systems, 2nd Edition. Springer, Berlin.

Wiggins, S., 1990. Introduction to Applied Nonlinear Dynamical Systems and Chaos. Springer, New York.